Polarization entanglement of sum-frequency photons: A tool to probe the Markovian limit

Victor Volkov[1,*] and Riccardo Chelli[2]

[1]*Bereozovaya 2A, Konstantinovo, Moscow Region 140207, Russian Federation*

[2]*Dipartimento di Chimica, Università di Firenze, Via della Lastruccia 3, I-50019 Sesto Fiorentino, Italy*

(Received 20 March 2015; published 24 June 2015)

The article addresses the possibility of entanglement-specific infrared-visible sum-frequency generation spectroscopy. In the case of an anisotropic interface, it is possible to employ *SSS* and *PSS* polarizations to detect responses not only specific to χ_{YYY} and χ_{XYY} nonlinearities, but also to higher-order $\chi_{(YYY)(XYY)}$ and $\chi_{(XYY)(YYY)}$ nonlinearities. Using quantum mechanical studies of the rhenium complex $[Re(OH)_3(CO)_3]$ as a molecular model, we demonstrate that if such complexes would form an anisotropic orientational distribution at a surface, under the considered geometry and the polarization settings, we may prepare quantum correlated C = O vibrational states to emit polarization-entangled photons. Accordingly, we explore the possibility of a polarization-measurement protocol to extract spectral signatures of the entangled states. The response would be informative on intramolecular interactions. As a result, we discuss the possible practical implications in probing dynamics at interfaces, and different opportunities in the preparation of entangled vibrational states of quantified fidelity.

DOI: 10.1103/PhysRevA.91.063831 PACS number(s): 42.65.−k, 03.67.Mn, 03.65.Ud

I. INTRODUCTION

Nonlinear spectroscopy, using sequences of ultrafast pulses, provides a powerful opportunity to explore the dynamics of quantum states and their correlations. In fact, the elucidation of relaxation mechanisms and correlations on a femtosecond time scale, both in the infrared [1] and in the visible [2] fields, has been the center of attention for the last 15 years. Entanglement is a quantum correlation, which may bypass locality [3]. It has to be considered whenever a wave function of N two-level systems or quantum information bits (qubits) may not be factorized as a tensor product [4]. In principle, this provides a 2^N capacity to store information [5]. Quantum computing stimulates the development of silicon chip technology [6–8], the ion trap technique [9], and the engineering of rotational [10–12] and/or vibrational packets [13,14]. Furthermore, progress in the preparation of entangled photons [15,16] has stimulated interest in using them as a spectroscopic tool. Recently, Roslyak *et al.* [17] and Mukamel [18] suggested novel experimental schemes (of second and third order) to characterize the structure and dynamics according to quantum correlations probed with entangled photons. This article pursues a different perspective: rather than using entangled photons, we focus on the phenomenon itself. Entanglement, if present, reports on the nature of a quantum state, as a mathematical object in Hilbert space. In fact, Bell states are the eigenstates of an interaction Hamiltonian, when it includes tensors product of σ_X and σ_Y Pauli operators [19]. In other words, once intermodal interactions are included, entanglement is present, unless the expected spectral signatures of intermodal relations are "erased" by the Markov limit.

Here, we address detection of polarization-entangled photons generated via infrared-visible sum-frequency generation (IR-VIS SFG), which is specific to structural motifs and dynamics at interfaces [20–23]. In this respect, there are two questions to be accounted for. First, can entanglement of IR-VIS SFG photons be securely detected? Second, if yes, then how informative and helpful can the entanglement spectrum be?

The outline of the article is the following. Section II describes the geometry of nonlinear experiments, the content (in terms of contributing nonlinearities) of second-order signals under different polarizations, the theory of detection of polarization-entangled two-photon states, and the molecular model system used to test the concept. In Sec. III, we explore the results of theoretical studies and discuss possible implications of IR-VIS SFG entanglement spectroscopy.

II. THEORY AND METHODS

A. IR-VIS SFG experiment: geometry and responses

In order to illustrate the approach, we address first the properties of the second-order IR-VIS SFG process on the basis of the interaction Hamiltonian $H^{\rm Int} = \hbar\, B^\dagger_{\rm SFG} B_{\rm VIS} B_{\rm IR}$, where B and $B^\dagger$ are the boson annihilation and creation operators. In lossless centrosymmetric media, most of the 27 elements of its third-order tensor become degenerate and average to zero [24]. However, an anisotropic interface would allow sampling contributions of most of its elements under the geometry shown in Fig. 1. When the infrared and visible beams are in the ZX plane, solving the equation

$$\frac{\lambda_{\rm VIS}}{\lambda_{\rm IR}} \sin[\beta_{\rm IR}] + \sin[\beta_{\rm VIS}] = 0, \tag{1}$$

where $\lambda_{\rm VIS}$ and $\lambda_{\rm IR}$ are the wavelengths, it is possible to search for such pairs of angles of incidence for two radiations ($\beta_{\rm VIS}$ and $\beta_{\rm IR}$), under which the SFG signal at the frequency $\omega_{\rm IR} + \omega_{\rm VIS}$ would be emitted exactly along the Z axis. A microscope objective, as shown in Fig. 1, would be necessary if an area of the interface with an anisotropic distribution of structural moieties is of submicron dimensions.

Using conventional linear polarizers, the geometry described allows the sampling of eight polarization-specific signals: *SSS*, *PPP*, *SPP*, *PSP*, *PPS*, *PSS*, *SPS*, and *SSP*. Here, capital letters from left to right indicate the selected

*volkovskr@gmail.com

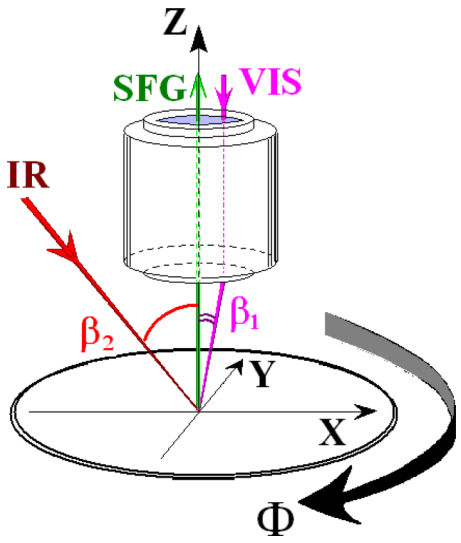

FIG. 1. (Color online) Experimental scheme.

polarizations for SFG, visible and infrared electromagnetic fields, respectively. S indicates that the electromagnetic field vector is along $\{0, 1, 0\}$. P implies that the electromagnetic field vector is in the incidence plane: thus, in general, the vector may have both X and Z components with respect to the laboratory frame. In general, one may expect the following contributions:

$$\begin{aligned}
SSS &: L_{yyy}\chi_{YYY}\mathbf{E}_Y\mathbf{E}_Y,\\
PPP &: L_{xxx}\chi_{XXX}\mathbf{E}_X\mathbf{E}_X + L_{zzz}\chi_{ZZZ}\mathbf{E}_Z\mathbf{E}_Z\\
&\quad + L_{xzz}\chi_{XZZ}\mathbf{E}_Z\mathbf{E}_Z + L_{zxx}\chi_{ZXX}\mathbf{E}_X\mathbf{E}_X\\
&\quad + L_{xzx}\chi_{XZX}\mathbf{E}_Z\mathbf{E}_X + L_{xxz}\chi_{XXZ}\mathbf{E}_X\mathbf{E}_Z\\
&\quad + L_{zxz}\chi_{ZXZ}\mathbf{E}_X\mathbf{E}_Z + L_{zzx}\chi_{ZZX}\mathbf{E}_Z\mathbf{E}_X,\\
SPP &: L_{yxx}\chi_{YXX}\mathbf{E}_X\mathbf{E}_X + L_{yzz}\chi_{YZZ}\mathbf{E}_Z\mathbf{E}_Z\\
&\quad + L_{yzx}\chi_{YZX}\mathbf{E}_Z\mathbf{E}_X + L_{yxz}\chi_{YXZ}\mathbf{E}_X\mathbf{E}_Z,\\
PSP &: L_{xyx}\chi_{XYX}\mathbf{E}_Y\mathbf{E}_X + L_{zyz}\chi_{ZYZ}\mathbf{E}_Y\mathbf{E}_Z\\
&\quad + L_{zyx}\chi_{ZYX}\mathbf{E}_Y\mathbf{E}_X + L_{xyz}\chi_{XYZ}\mathbf{E}_Y\mathbf{E}_Z,\\
PPS &: L_{xxy}\chi_{XXY}\mathbf{E}_X\mathbf{E}_Y + L_{zzy}\chi_{ZZY}\mathbf{E}_Z\mathbf{E}_Y\\
&\quad + L_{zxy}\chi_{ZXY}\mathbf{E}_X\mathbf{E}_Y + L_{xzy}\chi_{XZY}\mathbf{E}_Z\mathbf{E}_Y,\\
PSS &: L_{xyy}\chi_{XYY}\mathbf{E}_Y\mathbf{E}_Y + L_{zyy}\chi_{ZYY}\mathbf{E}_Y\mathbf{E}_Y,\\
SPS &: L_{yxy}\chi_{YXY}\mathbf{E}_X\mathbf{E}_Y + L_{yzy}\chi_{YZY}\mathbf{E}_Z\mathbf{E}_Y,\\
SSP &: L_{yyx}\chi_{YYX}\mathbf{E}_Y\mathbf{E}_X + L_{yyz}\chi_{YYZ}\mathbf{E}_Y\mathbf{E}_Z, \qquad (2)
\end{aligned}$$

where, the L-functions account for the local field contributions [25–30]. $\mathbf{E}_X$, $\mathbf{E}_Y$, and $\mathbf{E}_Z$ are the components of the electromagnetic field vectors: the left component in a product pair corresponds to the visible field and the right one to the infrared field. Also, it is important to note that for IR-VIS SFG nonlinearities, the tensor χ_{ijk} is invariant under the interchange of the first two indexes: for example, $\chi_{XYZ} = \chi_{YXZ}$. However, this symmetry relationship does not hold for the L-functions, namely, $L_{xyz} \neq L_{yxz}$.

Let us consider the case of a single resonance at $\omega_{\mathrm{IR}} + \omega_{\mathrm{VIS}}$, the signal of which satisfies Eq. (1) and is emitted strictly along the Z axis. Under such a condition, due to the loss of the Z components for the emitted responses, the content of the signals reduces to

$$\begin{aligned}
SSS &: L_{yyy}\chi_{YYY}\mathbf{E}_Y\mathbf{E}_Y,\\
PPP &: L_{xxx}\chi_{XXX}\mathbf{E}_X\mathbf{E}_X + L_{xzz}\chi_{XZZ}\mathbf{E}_Z\mathbf{E}_Z\\
&\quad + L_{xzx}\chi_{XZX}\mathbf{E}_Z\mathbf{E}_X + L_{xxz}\chi_{XXZ}\mathbf{E}_X\mathbf{E}_Z,\\
SPP &: L_{yxx}\chi_{YXX}\mathbf{E}_X\mathbf{E}_X + L_{yzz}\chi_{YZZ}\mathbf{E}_Z\mathbf{E}_Z\\
&\quad + L_{yzx}\chi_{YZX}\mathbf{E}_Z\mathbf{E}_X + L_{yxz}\chi_{YXZ}\mathbf{E}_X\mathbf{E}_Z,\\
PSP &: L_{xyx}\chi_{XYX}\mathbf{E}_Y\mathbf{E}_X + L_{xyz}\chi_{XYZ}\mathbf{E}_Y\mathbf{E}_Z,\\
PPS &: L_{xxy}\chi_{XXY}\mathbf{E}_X\mathbf{E}_Y + L_{xzy}\chi_{XZY}\mathbf{E}_Z\mathbf{E}_Y,\\
PSS &: L_{xyy}\chi_{XYY}\mathbf{E}_Y\mathbf{E}_Y,\\
SPS &: L_{yxy}\chi_{YXY}\mathbf{E}_X\mathbf{E}_Y + L_{yzy}\chi_{YZY}\mathbf{E}_Z\mathbf{E}_Y,\\
SSP &: L_{yyx}\chi_{YYX}\mathbf{E}_Y\mathbf{E}_X + L_{yyz}\chi_{YYZ}\mathbf{E}_Y\mathbf{E}_Z. \qquad (3)
\end{aligned}$$

However, if there is another spectrally narrow resonance at a different frequency $\omega_{\mathrm{IR},2} + \omega_{\mathrm{VIS},2}$, then it would not fulfill the direction of emission along the Z axis. It would emit into a different direction and the content of its signals would be given by Eq. (2).

The detection of phase-matched patterns of complex polarization content according to the spectral diversity of structural states (of different nonlinear responsivity) at interfaces is an interesting research direction. However, as a first approach, we may adopt a spectrally universal geometry, in which $\beta_{\mathrm{VIS}} = \beta_{\mathrm{IR}}$. For anisotropic interfaces, this implies a further simplification:

$$\begin{aligned}
&SSS : L_{yyy}\chi_{YYY}\mathbf{E}_Y\mathbf{E}_Y \quad \text{and} \quad PSS : L_{xyy}\chi_{XYY}\mathbf{E}_Y\mathbf{E}_Y,\\
&SPP : L_{yxx}\chi_{YXX}\mathbf{E}_X\mathbf{E}_X \quad \text{and} \quad PPP : L_{xxx}\chi_{XXX}\mathbf{E}_X\mathbf{E}_X,\\
&SSP : L_{yyx}\chi_{YYX}\mathbf{E}_Y\mathbf{E}_X \quad \text{and} \quad PSP : L_{xyx}\chi_{XYX}\mathbf{E}_Y\mathbf{E}_X,\\
&SPS : L_{yxy}\chi_{YXY}\mathbf{E}_X\mathbf{E}_Y \quad \text{and} \quad PPS : L_{xxy}\chi_{XXY}\mathbf{E}_X\mathbf{E}_Y. \qquad (4)
\end{aligned}$$

Here, we group signals into pairs on the basis of the orientation of the analyzer (S–P flip of the first index from the left). For example, under the geometry $\beta_{\mathrm{VIS}} = \beta_{\mathrm{IR}}$, if we employ the PSS polarization setting, we may detect the second-order SFG nonlinearity χ_{XYY}. Consistently, rotating the analyzer to the SSS setting, the signal would report on the χ_{YYY} nonlinearity. It is worth stressing here again that effective expressions for the χ_{XYY} and χ_{YYY} nonlinear responses require in-plane anisotropy, otherwise both, χ_{XYY} and χ_{YYY} average to zero [24]. Finally, employment of a spectrometer allows spectral characterization of both nonlinearities, through their dependences on the frequencies of the contributing resonances. Thus, we may rely on the following requirements: (i) for a simple example, we will consider a pair of two-level oscillators with distinct (spectrally resolvable) resonances; (ii) the oscillators are distributed anisotropically at the surface; and (iii) both oscillators are Raman or IR active to secure effective IR-VIS SFG.

B. Detection of polarization entanglement

In order to approach SFG spectroscopy in the described system, we need to review and adopt the Jones matrix formalism to characterize the polarization states of the detected

photonic states. In particular, for single photons specific to χ_{YYY} and χ_{XYY} nonlinearities at two different frequencies ω_1 and ω_2, we introduce the following notation:

$$|YYY_1\rangle = \begin{bmatrix}1\\0\end{bmatrix}_1 \quad \text{and} \quad |YYY_2\rangle = \begin{bmatrix}1\\0\end{bmatrix}_2, \tag{5}$$

$$|XYY_1\rangle = \begin{bmatrix}0\\1\end{bmatrix}_1 \quad \text{and} \quad |XYY_2\rangle = \begin{bmatrix}0\\1\end{bmatrix}_2. \tag{6}$$

To test a state (upon detection), we adopt the following analyzing operators:

$$\mathbb{P}_{YYY,1} = \begin{bmatrix}1&0\\0&0\end{bmatrix}_1 \quad \text{and} \quad \mathbb{P}_{YYY,2} = \begin{bmatrix}1&0\\0&0\end{bmatrix}_2, \tag{7}$$

$$\mathbb{P}_{XYY,1} = \begin{bmatrix}0&0\\0&1\end{bmatrix}_1 \quad \text{and} \quad \mathbb{P}_{XYY,2} = \begin{bmatrix}0&0\\0&1\end{bmatrix}_2. \tag{8}$$

These correspond to orientations of the analyzer that allow the passage of perpendicular and parallel (with respect to the incident plane) polarized emitted photons at one of the two frequencies as indicated by the subscripts. Accordingly, an analyzing matrix to describe a 45° oriented analyzer can be prepared as follows:

$$\mathbb{P}_{45,1} = \tfrac{1}{2}\begin{bmatrix}1&0\\0&0\end{bmatrix}_1 + \tfrac{1}{2}\begin{bmatrix}0&0\\0&1\end{bmatrix}_1 \quad \text{and}$$
$$\mathbb{P}_{45,2} = \tfrac{1}{2}\begin{bmatrix}1&0\\0&0\end{bmatrix}_2 + \tfrac{1}{2}\begin{bmatrix}0&0\\0&1\end{bmatrix}_2. \tag{9}$$

The subscript sorts a matrix acting on its own frequency subspace. Further, we will apply the formalism to address the possibility of sensing vibrational entanglement at interface.

Using the description of analyzing operators, we express the probability of observing a nonlinear emitted photon of arbitrary polarization. By acting on a superposition of kets, we obtain

$$\begin{aligned}&\mathbb{P}_{YYY,1}\mathbb{P}_{YYY,2}(|YYY_1\rangle + |YYY_2\rangle + |XYY_1\rangle + |XYY_2\rangle)\\ &\quad = 1|YYY_1\rangle + 1|YYY_2\rangle.\end{aligned} \tag{10}$$

Exploiting the product with the incoming photons expressed in bra vector notation, unit contributions of χ_{YYY} nonlinearities are confirmed. Analogously, using an analyzer with its axis oriented parallel to the incidence plane, we obtain unit contributions of χ_{XYY} nonlinearities,

$$\begin{aligned}&\mathbb{P}_{XYY,1}\mathbb{P}_{XYY,2}(|YYY_1\rangle + |YYY_2\rangle + |XYY_1\rangle + |XYY_2\rangle)\\ &\quad = 1|XYY_1\rangle + 1|XYY_2\rangle.\end{aligned} \tag{11}$$

The probabilities when the analyzer is set to 45° are obtained from

$$\begin{aligned}&\mathbb{P}_{45,1}\mathbb{P}_{45,2}(|YYY_1\rangle + |YYY_2\rangle + |XYY_1\rangle + |XYY_2\rangle)\\ &\quad = \tfrac{1}{2}|YYY_1\rangle + \tfrac{1}{2}|YYY_2\rangle + \tfrac{1}{2}|XYY_1\rangle + \tfrac{1}{2}|XYY_2\rangle.\end{aligned} \tag{12}$$

The usual multiplication of Eq. (12) by the incoming photons in bra vector notation confirms a probability of one-half for each nonlinearity. The important implication of these observations is that a measurement with the analyzer geometry at 45° is equal to half of the sum of two measurements taken under parallel and perpendicular (with respect to the incidence plane) orientations of the analyzer.

Now, let us consider the implication of polarization-sensitive detection for two-photon states, which can be described as

$$\begin{aligned}&|XYY_1XYY_2\rangle, \quad |YYY_1YYY_2\rangle,\\ &|YYY_1XYY_2\rangle, \quad |XYY_1YYY_2\rangle.\end{aligned} \tag{13}$$

Here, we make no assumption on the origin of the two-photon states, leaving this to the discussion. The considered algebra for polarized states is analogous to that of sigma and tau spin operators for $|ab\rangle$ two-electron states in the Bell experiment [31]. The probabilities of observation with the analyzer oriented perpendicular to the incidence plane are

$$\begin{aligned}P_1 &= \langle XYY_1XYY_2|\mathbb{P}_{YYY,1}\mathbb{P}_{YYY,2}|XYY_1XYY_2\rangle\\ &= \langle XYY_1XYY_2|0_10_2\rangle = 0,\\ P_2 &= \langle YYY_1YYY_2|\mathbb{P}_{YYY,1}\mathbb{P}_{YYY,2}|YYY_1YYY_2\rangle\\ &= \langle YYY_1YYY_2|YYY_1YYY_2\rangle = 1_{YYY,1}1_{YYY,2},\\ P_3 &= \langle YYY_1XYY_2|\mathbb{P}_{YYY,1}\mathbb{P}_{YYY,2}|YYY_1XYY_2\rangle\\ &= \langle YYY_1XYY_2|YYY_10_2\rangle = 0,\\ P_4 &= |XYY_1YYY_2\rangle\mathbb{P}_{YYY,1}\mathbb{P}_{YYY,2}|XYY_1YYY_2\rangle\\ &= \langle XYY_1YYY_2|\,0_1YYY_2\rangle\ = 0,\end{aligned} \tag{14}$$

where the subscripts of the probabilities, for example, in $1_{YYY,1}1_{YYY,2}$, indicate both the nature and the polarization character of the states. Analogously, probabilities of observation with the axis of the analyzer oriented parallel to the incidence plane are

$$\begin{aligned}P_5 &= \langle XYY_1XYY_2|\mathbb{P}_{XYY,1}\mathbb{P}_{XYY,2}|XYY_1XYY_2\rangle\\ &= \langle XYY_1XYY_2|XYY_1XYY_2\rangle = 1_{XYY,1}1_{XYY,2},\\ P_6 &= \langle YYY_1\ YYY_2|\mathbb{P}_{XYY,1}\mathbb{P}_{XYY,2}|YYY_1YYY_2\rangle\\ &= \langle YYY_1YYY_2|0_10_2\rangle = 0,\\ P_7 &= \langle YYY_1XYY_2|\mathbb{P}_{XYY,1}\mathbb{P}_{XYY,2}|YYY_1XYY_2\rangle\\ &= \langle YYY_1XYY_2|0_1XYY_2\rangle = 0,\\ P_8 &= \langle XYY_1YYY_2|\mathbb{P}_{XYY,1}\mathbb{P}_{XYY,2}|XYY_1YYY_2\rangle\\ &= \langle XYY_1YYY_2|XYY_10_2\rangle = 0.\end{aligned} \tag{15}$$

Consistently, the probabilities of observing photon emission with the axis of the analyzer oriented at 45° are

$$\begin{aligned}P_9 &= \langle XYY_1XYY_2|\mathbb{P}_{45,1}\mathbb{P}_{45,2}|XYY_1XYY_2\rangle\\ &= \tfrac{1}{2}{}_{XYY,1}\tfrac{1}{2}{}_{XYY,2},\\ P_{10} &= \langle YYY_1YYY_2|\mathbb{P}_{45,1}\mathbb{P}_{45,2}|YYY_1YYY_2\rangle\\ &= \tfrac{1}{2}{}_{YYY,1}\tfrac{1}{2}{}_{YYY,2},\\ P_{11} &= \langle YYY_1XYY_2|\mathbb{P}_{45,1}\mathbb{P}_{45,2}|YYY_1XYY_2\rangle\\ &= \tfrac{1}{2}{}_{YYY,1}\tfrac{1}{2}{}_{XYY,2},\\ P_{12} &= \langle XYY_1YYY_2|\mathbb{P}_{45,1}\mathbb{P}_{45,2}|XYY_1YYY_2\rangle\\ &= \tfrac{1}{2}{}_{XYY,1}\tfrac{1}{2}{}_{\ YYY,2}.\end{aligned} \tag{16}$$

Here, it is important to note that a spectral response of two-photon states shows up as double-hump spectral signature, where each hump is specific to one of the resonances. The contribution of nonlinearities to each resonance is according to the indicated probability. However, factoring a doublet (if observed) into single resonance contributions would be improper. The considered spectra of the entangled photons would include signatures of both resonances. A use of a chromatic optics to split spectral components of the entangled states would be identical to a measurement.

Next, we consider the difference between a measurement with analyzer set to 45° and half the sum of two measurements with the analyzer set parallel and perpendicular to the incidence plane. This is somewhat analogous to the witness operator formalism [32]; there, the one-photon manifold does not contribute to such difference. Considering evaluations of the integrals $P_1 \div P_{12}$, the difference would yield a pair of two-photonic states compositions:

$$\begin{aligned} &P_9 + P_{10} + P_{11} + P_{12} - 0.5\,(P_2 + P_5) \\ &\quad = \langle YYY_1XYY_2|\mathbb{P}_{45,1}\mathbb{P}_{45,2}|YYY_1XYY_2\rangle \\ &\qquad + \langle XYY_1YYY_2|\mathbb{P}_{45,1}\mathbb{P}_{45,2}|XYY_1YYY_2\rangle \\ &\quad = \tfrac{1}{2}_{YYY,1}\tfrac{1}{2}_{XYY,2} + \tfrac{1}{2}_{XYY,1}\tfrac{1}{2}_{YYY,2}. \end{aligned} \tag{17}$$

The subtraction procedure would ensure elimination of the local field factors and instrumental contributions due to the properties of the analyzer, spectrometer, and detector. The extraction of the signal would therefore be possible in the presence of entanglement. Thus, the suggested treatment answers the first question: how to determine unambiguously if polarization entanglement is present. We may call the spectral contribution of Eq. (17) an "information-sharing" term.

C. Molecular system

To illustrate the described nonlinear phenomenon, we consider a surface with an anisotropic distribution of rhenium complexes, $[Re(OH)_3(CO)_3]$. For example, the (001) surface of Al_2O_3 or the (111) surface of MgO has either three- or sixfold symmetry [33]. Accordingly, it is reasonable to expect possible anisotropic distributions of rhenium complexes at such crystalline surfaces [34,35]. To compute the optimized structure, vibrational frequencies, transition dipole moments, and Raman tensors of the complex, we have employed density functional theory implemented in the GAUSSIAN09 package [36] with the restricted B3LYP exchange-correlation functional [37,38] at the LanL2DZ level of theory.

Figure 2 provides a graphical representation of the complex at the surface with a structural reference to describe the orientation. Additionally, it indicates the atomic displacements of antisymmetric and symmetric stretching modes of carbonyls, which peak at 1942 and 1972 cm^{-1}, respectively. Using the computed transition dipole moments and Raman tensors specific to these carbonyl modes, we have calculated the macroscopic nonlinearities in dependence on the orientation of the complex. The integration protocol to obtain nonlinearities as angular functions is provided elsewhere [39].

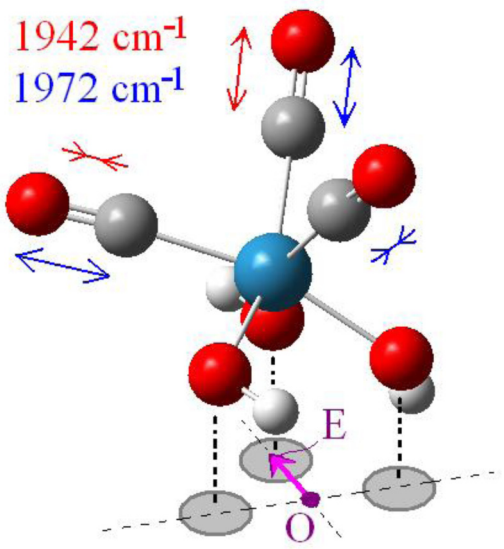

FIG. 2. (Color online) Rhenium complex considered at a crystalline surface according to Ref. [34]. We adopt the orientation when the oxygen atoms of the OH groups form a plane parallel to the surface. The black dashed lines indicate projections of the oxygen atoms on the surface (XY plane of the laboratory frame; see also Fig. 1). The magenta OE vector, which connects the middle of the line between the surface projections of the two oxygens and the projection of the third oxygen (as shown), is the reference vector. We use it to represent the dependence of the nonlinear intensities on the angle between OE and the X axis of the laboratory frame. Red and blue arrows indicate relative displacements of C = O moieties specific to the normal modes with frequencies at 1942 and 1972 cm^{-1}.

III. RESULTS AND DISCUSSION

In the preceding section, we have described the conditions for the detecting of spectral signatures specific to polarization-entangled photons formed upon an IR-VIS SFG process at an anisotropic interface. Hence, now we need to establish how informative the response could be in the characterization of a material system. Copropagation of photons, generated through second-order nonlinear responses, may lead to the formation of two-photon correlated pairs [40,41]. Moreover, Nagasako *et al.* [15] demonstrated that the recombination of such pairs is a useful approach to engineer Bell states. However, considering the density of suitable vibrational states at a surface, here we disregard intermolecular interactions to correlate second-order SFG photons [42]. To account for the suggested entanglement, we assume that the generation of two photons, at frequencies $\omega_{IR1} + \omega_{VIS}$ and $\omega_{IR2} + \omega_{VIS}$, takes place on the same molecule.

To address the time evolution of the system, where sum-frequency excitations of two normal modes take place on the same metal cluster, we adopt the Keldysh-Schwinger formalism [17,43]. In this case, bra and ket sides describe contributions of two normal modes, respectively, as shown in Fig. 3. Following Mukamel [44], we may write the response

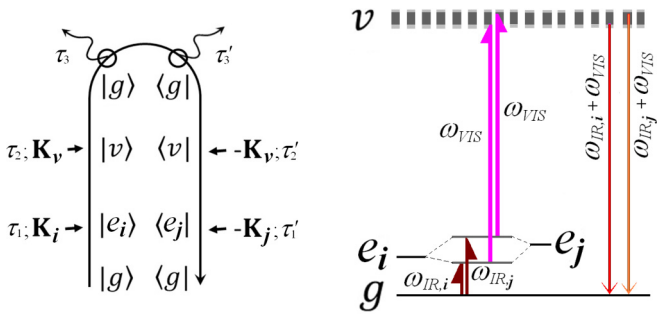

FIG. 3. (Color online) Keldysh integration contour for two-photon emission IR-VIS SFG processes specific to a pair of C = O normal modes of a rhenium cluster, and the corresponding level diagram.

function in Hilbert space as

$$
\begin{aligned}
&R(\tau_3',\tau_2',\tau_1',\tau_1,\tau_2,\tau_3)\\
&\quad=\left(\frac{i}{\hbar}\right)^4\langle G(\tau_3',\tau_2',\tau_1')\cdot\ G(\tau_1,\tau_2,\tau_3)\rangle,\\
&G(\tau_3',\tau_2',\tau_1')\\
&\quad=e^{-\frac{i}{\hbar}H_g\tau_3'}\mu_{\mathrm{IR2}}(\tau_3')e^{\frac{i}{\hbar}H_{e_2}\tau_3'}e^{-\frac{i}{\hbar}H_{e_2}\tau_2'}\mu_{\mathrm{VIS}}(\tau_2')\\
&\qquad\times e^{\frac{i}{\hbar}H_v\tau_2'}e^{-\frac{i}{\hbar}H_v\tau_1'}\mu_{\mathrm{SF2}}(\tau_1')e^{\frac{i}{\hbar}H_g\tau_1'},\\
&G(\tau_1,\tau_2,\tau_3)\\
&\quad=\ e^{\frac{i}{\hbar}H_g\tau_1}\mu_{\mathrm{SF1}}(\tau_1)e^{-\frac{i}{\hbar}H_v\tau_1}e^{\frac{i}{\hbar}H_v\tau_2}\mu_{\mathrm{VIS}}(\tau_2)\\
&\qquad\times e^{-\frac{i}{\hbar}H_{e_1}\tau_2}e^{\frac{i}{\hbar}H_{e_1}\tau_3}\mu_{\mathrm{IR1}}(\tau_3)e^{-\frac{i}{\hbar}H_g\tau_3}.
\end{aligned}
\tag{18}
$$

Here, the angular brackets determine the time-correlation function. $\tau_3=0$, $\tau_1=\mathrm{t}_1$, $\tau_2=\mathrm{t}_1+\mathrm{t}_2$, and $\tau_3'=0$, $\tau_1'=\mathrm{t}'_1,\tau_2'=\mathrm{t}'_1+\mathrm{t}'_2$, where t'_1 and t'_2 are negative times that provide backward evolution along the bra side. Also, considering that visible excitations are nonresonant, we set $\mathrm{t}_2=0$ and $\mathrm{t}'_2=0$. Hence, $\alpha_{\mathrm{SF1}}(t_1)=\ \mu_{\mathrm{SF1}}(t_1)\mu_{\mathrm{VIS}}(t_1)$ and $\alpha_{\mathrm{SF2}}(t_1')=\mu_{\mathrm{SF2}}(t_1')\mu_{\mathrm{VIS}}(t_1')$. As a result, we may rewrite the response function

$$
\begin{aligned}
R(t_1',t_1)=\left(\frac{i}{\hbar}\right)^4\Big\langle&\mu_{\mathrm{IR2}}e^{-\frac{i}{\hbar}H_{e_2}t_1'}\alpha_{\mathrm{SF2}}(t_1')e^{\frac{i}{\hbar}H_g(t_1'+\ t_1)}\\
&\times\alpha_{\mathrm{SF1}}(t_1)e^{-\frac{i}{\hbar}H_{e_1}t_1}\mu_{\mathrm{IR1}}\Big\rangle.
\end{aligned}
\tag{19}
$$

Stemming from the commutation relations of the memory kernel in the master equation, the results of diagrammatic studies [45] suggest that the two-color entanglement would manifest itself directly on anharmonic terms of the intermodal interaction, Φ_{iij} and Φ_{ijj}, where the i and j indexes correspond to the two modes. In fact, upon subtraction, as shown in Eq. (17), the residual term provides spectral signatures, which is strictly specific to the case when both normal modes are excited: the protocol implies subtraction of the spectral signatures of the responses when each mode is excited alone (uncorrelated).

Four operators, along the integration contour, suggest scaling of the response in Eq. (19) with susceptibility χ_{XYYYYY}; see Sec. 6B in Ref. [42]. To understand the nature of the correlation of the signals better, we explore χ_{XYY}, χ_{YYY}, χ_{XYYYYY}, and

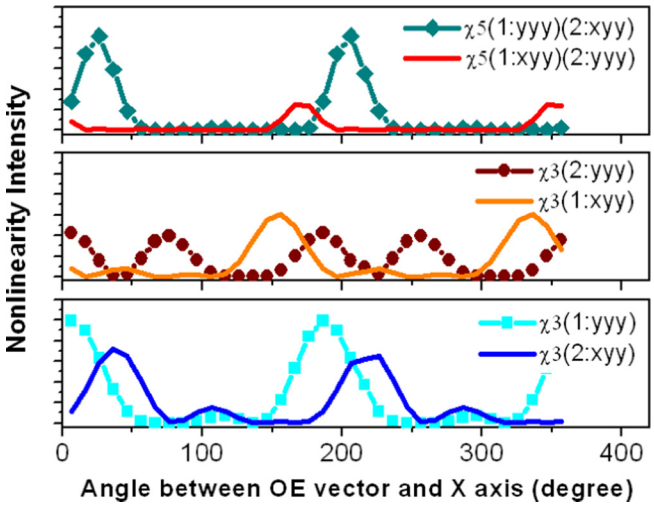

FIG. 4. (Color online) The dependence of the intensities of the second-order, χ_{YYY} and χ_{XYY}, and the fifth-order, $\chi_{(YYY)(XYY)}$ and $\chi_{(XYY)(YYY)}$, nonlinearities specific to one and another resonance on the angle between the OE vector (see Fig. 2) and the X axis of the laboratory frame. The numbers 1 and 2 in the legend correspond to the normal modes at 1942 and 1972 cm^{-1}, respectively. In the case of the fifth-order nonlinearities, the two triplets of indexes are specific to different resonances as indicated in the legend.

χ_{YYYXYY} nonlinearities through their dependences on the angle of orientation of the complex: see Fig. 4. The nonlinearities are expressed at instantaneous limit. The numerical values are according to the integration protocol described earlier [39]. As a first approach, adopting the instantaneous limit is reasonable since the time variance of the response function would be according to the time duration of the second (visible) excitation.

Optical properties, as expressed in Fig. 4, are determined for a rhenium complex coordinated to a surface with its three oxygen atoms (of OH groups) forming a plane parallel to the surface. Next, we express the second-order χ_{YYY} and χ_{XYY} nonlinear intensities specific to the normal modes at 1942 and 1972 cm^{-1} in their dependences on the angle between the OE reference vector and the X axis of the laboratory frame (see Fig. 2). In particular, the cyan square line and brown circle line show angular dependencies of the χ_{YYY} tensor elements of antisymmetric and symmetric equatorial metal carbonyl stretchings, respectively. Analogously, orange and blue lines would help to predict the surface anisotropy of the χ_{XYY} responses for the same modes. In principle, the angular dependencies of the intensities (the contrast by ratio of maximal and maximal readings) may provide information on the anisotropy of the preferred orientation of the complexes and on the reorientation dynamics (through smearing upon averaging). Of course, the main interest of this work is to understand higher-order correlations. Considering the two terms in Eq. (17), in Fig. 4 we compare two nonlinearities. One is related to $\chi_{(YYY)(XYY)}$, where the subscript YYY reflects the hyperpolarizabilities of the lower-frequency mode and the subscript XYY is specific to the higher-frequency symmetric equatorial stretching. The other nonlinearity is characteristic to surface anisotropy and corresponds to $\chi_{(XYY)(YYY)}$. The

two dependencies of the entangled responses relate to the corresponding second-order contributions. We see that the $\chi_{(XYY)(YYY)}$ peak at about 180° correlates with the nonlinearities χ_{XYY} and χ_{YYY} of the normal modes at 1942 and 1972 cm^{-1}, respectively, as reported in the middle panel of Fig. 4. Analogously, the $\chi_{(YYY)(XYY)}$ nonlinear intensity at 210° correlates fairly well with the χ_{YYY} and χ_{XYY} of the normal modes at 1942 and 1972 cm^{-1}, respectively (see bottom panel of Fig. 4). Overall, the higher nonlinear intensities around 10° and 190°(±20°) occur because, under such orientations, the displacements of the equatorial C = O moieties are the most parallel to the Y axis of the laboratory frame. The anticipated dependencies of the high-order correlations suggest that for the two stretching modes of the complex, the $|YYY_1XYY_2\rangle$ contribution in Eq. (13) is dominant, and that may be confirmed, optimized, and even rectified by the angle Φ of the sample rotation: see Fig. 1. Furthermore, considering the $|YYY_1XYY_2\rangle$ and $|XYY_1YYY_2\rangle$ terms as the $|01\rangle$ and $|10\rangle$ components, we may establish a Bell state at $\Phi = 181°$.

It is important to address here that the explored susceptibilities are computed at the instantaneous limit. Accounting of time dependences (dynamics) may lead to smearing of the entanglement responses or even to their decay, when the probed resonances are specific to structural moieties, which undergo a rapid (on the time scale of the pulses' duration) structural reorientation and/or rearrangement. This provides an opportunity to test entanglement enhancement upon a motional narrowing in a temperature-dependent experiment. In other words, an observation of two-resonant spectral signatures would be possible as long as the dynamics of the system is non-Markovian on the time scale of the emission-detection time window. For example, in a recent theoretical study concerning non-Markovian effects on entanglement between two modes interacting with an Ohmic bath, the results indicate that (under all regimes) the Markovian limit enhances a rapid decay of the correlations [46]. The approach could be particularly insightful in the elucidation of structural and dynamic relations between dangling and bound stretching modes at crystalline surfaces [47,48], and in paired states under effective coupling [49].

Finally, it is important to notice that the suggested detection of spectral signature specific to entangled states may provide the necessary condition for the quantitative characterization of the modes under quantum correlations. The suggested experimental approach provides the necessary input to search for an optimal measurement scheme for a quantum state tomography [50]. If accomplished, this would lead to a quantitative characterization of the corresponding density matrix.

IV. CONCLUSIONS

In this work, we suggest an experimental approach aimed to observe polarization entanglement of photonic states in IR-VIS SFG spectroscopy. Specifically, the article explores theoretically possible quantum correlations of photons using nonlinearities of carbonyl stretching modes of the rhenium complex $[Re(OH)_3(CO)_3]$, which may form an anisotropic distribution upon coordination to an oxide surface. Quantum mechanical calculations combined with orientational averaging studies suggest that under the *SSS* and the *PSS* polarizations (a pair of settings among several possible combinations), photon correlations can be possible due to the $\chi_{(YYY)(XYY)}$ and/or $\chi_{(XYY)(YYY)}$ nonlinearities. Furthermore, rotation of the sample plane (with oriented metal complexes) with respect to the laboratory frame may help suppress the relatively weaker $\chi_{(XYY)(YYY)}$ nonlinearity to yield the dominant $\chi_{(YYY)(XYY)}$ contribution. The described experimental geometry and the signal extraction protocol offer a different approach to probe structural and orientation dynamics at interfaces: quantum correlation is expected to decay fast at the Markovian limit. Finally, the approach may provide a valuable opportunity to design and test entangled vibrational states (at interfaces) of quantified fidelity.

ACKNOWLEDGMENT

V.V. thanks Dr. Alexei Maradudin, School of Physical Sciences at the University of California, Irvine, for encouragement and helpful discussion.

[1] M. Asplund, M. Zanni, and R. Hochstrasser, Proc. Natl. Acad. Sci. USA **97**, 8219 (2000).
[2] G. S. Engel, T. R. Calhoun, E. L. Read, T. K. Ahn, T. Mancal, Y. C. Cheng, R. E. Blankenship, and G. R. Fleming, Nature (London) **446**, 782 (2007).
[3] C. K. Hong, and L. Mandel, Phys. Rev. A **31**, 2409 (1985).
[4] A. Einstein, B. Podolski, and N. Rosen, Phys. Rev. **47**, 777 (1935).
[5] R. Feynman, Intl. J. Theor. Phys. **21**, 467 (1982).
[6] L. DiCarlo, J. M. Chow, J. M. Gambetta, L. S. Bishop *et al.*, Nature (London) **460**, 240 (2009).
[7] A. Politi, J. Matthews, and J. O'Brien, Science **325**, 1221 (2009).
[8] K. L. Litvinenko, E. T. Bowyer, P. T. Greenland, N. Stavrias *et al.*, Nature Comm. **6**, 6549 (2015).
[9] J. I. Cirac and P. Zoller, Phys. Rev. Lett. **74**, 4091 (1995).
[10] Y. Y. Liao, Y. N. Chen, and D. S. Chuu, Chem. Phys. Lett. **398**, 418 (2004).
[11] E. Charron, P. Milman, A. Keller, and O. Atabek, Phys. Rev. A **75**, 033414 (2007).
[12] K. Shioya, K. Mishima, and K. Yamashita, Mol. Phys. **105**, 1283 (2007).
[13] C. Tesch, L. Kurtz, and R. de Vivie-Riedle, Chem. Phys. Lett. **343**, 633 (2001).
[14] D. Shyshlov, and D. Babikov, J. Chem. Phys. **137**, 194318 (2012).
[15] E. M. Nagasako, S. J. Bentley, R. W. Boyd, and G. S. Agarwal, Phys. Rev. A **64**, 043802 (2001).
[16] L. Mandel and E. Wolf, *Optical Coherence and Quantum Optics* (Cambridge University Press, Cambridge,1995).
[17] O. Roslyak, C. A. Marx, and S. Mukamel, Phys. Rev. A **79**, 033832 (2009).

[18] S. Mukamel. J. Chem. Phys. **132**, 241105 (2010).
[19] D. McMahon, *Quantum Computing Explained* (Wiley, Hoboken, NJ, 2008).
[20] X. D. Zhu, H. Suhr, and Y. R. Shen, Phys. Rev. B **35**, 3047 (1987).
[21] J. C. Conboy, M. C. Messmer, and G. L. Richmond, J. Phys. Chem. B **101**, 6724 (1997).
[22] G. Kim, M. Gurau, S. Lim, and P. Cremer, J. Phys. Chem. B **107**, 1403 (2003).
[23] H. Allen, N. Casillas-Ituarte, M. Sierra-Hernández, X. Chen, and C. Tang, Phys. Chem. Chem. Phys. **11**, 5538 (2009).
[24] D. A. Kleinman, Phys. Rev. **126**, 1977 (1962).
[25] J. E. Sipe, Surf. Sci. **105**, 489 (1981).
[26] B. Dick, A. Gierulski, G. Marowsky, and G. A. Reider, Appl. Phys. B **38**, 107 (1985).
[27] B. U. Felderhof, and G. Marowsky, Appl. Phys. B **44**, 11 (1987).
[28] C. Hirose, N. Akamatsu, and K. Domen, Appl. Spec. **46**, 1051 (1992).
[29] X. Zhuang, P. B. Miranda, D. Kim, and Y. R. Shen, Phys. Rev. B **59**, 12632 (1999).
[30] G. Li, A. Dhinojwala, and M. S. Yeganeh, J. Phys. Chem. C **115**, 7554 (2011).
[31] J. Clauser, M. Horne, A. Shimony, and R. A. Holt, Phys. Rev. Lett. **23**, 880 (1969).
[32] C.-M. Li, L.-Y. Hsu, Y.-N. Chen, D.-S. Chuu, and T. Brandes, Phys. Rev. A **76**, 032313 (2007).
[33] J. M. Thomas and W. J. Thomas, *Principles and Practice of Heterogeneous Catalysis* (John Willey & Sons, Weinheim, 2014).
[34] P. Kirlin, F. DeThomas, J. Bailey, H. Gold, C. Dybowski, and B. Gates, J. Phys. Chem. **90**, 4882 (1986).
[35] S. K. Purnell, X. Xu, D. W. Goodman, and B. C. Gates, Langmuir **10**, 3057 (1994).
[36] M. J. Frisch, G. W. Trucks, H. B. Schlegel, G. E. Scuseria, M. A. Robb, J. R. Cheeseman, G. Scalmani, V. Barone, B. Mennucci, G. A. Petersson *et al.*, *Gaussian 09, Revision A.1* (Gaussian, Inc.: Wallingford, CT, 2009).
[37] A. D. Becke, Phys. Rev. A **38**, 3098 (1988).
[38] C. Lee, W. Yang, and R. G. Parr, Phys. Rev. B **37**, 785 (1988).
[39] V. Volkov, J. Chem. Phys. **141**, 134121 (2014).
[40] L. Hardy, Phys. Lett. A **161**, 326 (1992).
[41] P. G. Kwiat, K. Mattle, H. Weinfurter, A. Zeilinger, A. V. Sergienko, and Y. Shih, Phys. Rev. Lett. **75**, 4337 (1995).
[42] O. Roslyak and S. Mukamel, Opt. Express **17**, 1093 (2009).
[43] S. Mukamel, Phys. Rev. E **68**, 021111 (2003).
[44] S. Mukamel, *Principles of Nonlinear Optical Spectroscopy* (Oxford University Press, Oxford, 1995).
[45] K. Okumura and Y. Tanimura, J. Chem. Phys. **106**, 1687 (1997).
[46] J.-H. An1, Y. Yeo, W.-M. Zhang, and C. H. Oh, J. Phys. A: Math. Theor. **42**, 015302 (2009).
[47] Y. R. Shen, Solid State Commun. **108**, 399 (1998).
[48] V. Buch, T. Tarbuck, G. L. Richmond, H. Groenzin, I. Li, and M. J. Shultz. J. Chem. Phys. **127**, 204710 (2007).
[49] V. Vasilets, G. Shandryuk, G. Savenkov, A. Shatalova, G. Bondarenko, R. Talroze, and N. Plate, Macromolecules **37**, 3685 (2004).
[50] M. Mohammadi and A. M. Branczyk, Phys. Rev. A **89**, 012113 (2014).